Use of Computational Fluid Dynamics to Reduce Particulate Emissions from Wood-Fired Hydronic Furnace

26

Paul E. Glanville[1], Michael J. Kirby[2], Advisor: Dr. John C. Kramlich[1]

1 University of Washington, 2 Greenwood Technologies LLC

Overview

We identify the sources of Particulate Matter (PM) emissions from a wood-fired hydronic furnace through the use of 2D and 3D Computation Fluid Dynamics (CFD) modeling. With a certified EPA Test Method 28 data set of a commercially available furnace, we benchmark several CFD simulation methods and compare their relative accuracies and computational expenses. While PM formation and oxidation is not modeled directly, due to the lack of a comprehensive model for Organic Carbon PM[1], **combustion efficiency and post-flame mixing are used as metrics of emissions reductions**. From this benchmarked set of modeling methods, we simulate several operational and physical modifications and then experimentally determine their effectiveness in reducing PM emissions without compromising thermal efficiency.

Introduction

The fixed-bed furnace used in this study, shown in a CFD model domain rendering in Figure 1 with a 'test crib' wood fuel charge, operates as follows:

- Natural draft preheated air enters four inlet tubes into the brick firebox
- Radiation to the wood load drives solid and gas phase pyrolysis
- Buoyant flames develop, drawing flue gases over 19 heat extraction water tubes, the exterior of the air preheat tubes, and out the stack

Figure 1: Furnace Interior and Thermocouple Locations

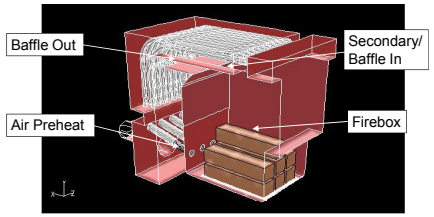

Wood is generally considered to burn in four distinct, but overlapping stages[2]: (1) heating and drying, (2) solid-phase pyrolysis, (3) gas phase pyrolysis and oxidation, and (4) char oxidation. Considering only the carbonaceous portion, PM from wood combustion is 90% Organic Carbon and 4% Black Carbon[3], with much of the former formed in the 3rd stage as a result of tars and other organic species escaping and condensing post-flame[4].

Assuming White Oak is $C_{4.12}H_{5.38}N_{0.03}O_{2.70}$[5] and product species are limited to CO, CO_2, N_2, O_2, and H_2O, initial stoichiometric analysis and observations suggest that the majority of PM emissions occur during the first 30 minutes (so-called 'peak pyrolysis') of the fuel-rich burn as seen in Figure 2. For these reasons and that CFD is well suited in modeling the turbulent reacting flow field, **this study focuses primarily on the gas phase pyrolysis and oxidation stage**. The 1st and 2nd stages have marked effects on pyrolysis rates, flame temperatures, and will be incorporated as boundary conditions and modeling assumptions.

Figure 2: Phi and Measured PM Emissions Rate During Initial Test

$$\varphi = \frac{\left(\dot{n}_{air}/\dot{n}_{fuel}\right)_{actual}}{\left(\dot{n}_{air}/\dot{n}_{fuel}\right)_{stoichiometric}}$$

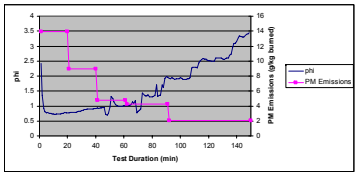

Benchmark Modeling

Using FLUENT version 6.3 with a grid consisting of 104,000 tetrahedral cells within the domain of Figure 1, the Favre-Averaged Navier Stokes equations are solved, along with enthalpy and species transport equations using finite volume discretization and SIMPLE pressure-velocity coupling and the k-ε turbulence model. Radiation exchange is modeled by the Discrete Transfer Radiation Model (DTRM), with the weighted-sum-of-gray-gases assumption[6].

Wood Chemistry

- Gas-phase pyrolysis species are modeled as a surrogate molecule CH_2O or as a mixture of CH_4, CO, CO_2, H_2, and H_2O (based upon known moisture content)[7,8]
- A solid-phase pyrolysis limited fuel flux is modeled as a zeroth order Arrhenius rate by the equation[9]:

$$\dot{m} = A_p S_A \rho e^{\left(-E/RT\right)}$$

Buoyancy-dominated Non-premixed Combustion

- Combustion is modeled using the mixture fraction model[10] or by the finite-rate/eddy-dissipation model[11] with the following four-step mechanism[8]:

$$CO + \frac{1}{2}O_2 \Rightarrow CO_2 \qquad H_2 + \frac{1}{2}O_2 \Rightarrow H_2O$$
$$CO + H_2O \Leftrightarrow CO_2 + H_2 \qquad CH_4 + 2O_2 \Rightarrow CO_2 + 2H_2O$$

•Loss of detail between 2D vs. 3D and steady state vs. transient is addressed.

Table 1: Benchmark Modeling Summary

Run	Simulation	Fuel	Turbulent Combustion Model
1	2D Steady	CH_2O	Mixture Fraction/PDF
2	3D Steady	CH_2O	Mixture Fraction/PDF
3	3D Steady	CH_2O	Mixture Fraction/PDF-pyrolysis limited
4	3D Steady	Mixture	Mixture Fraction/PDF
5	3D Unsteady	Mixture	Eddy-Dissipation

Boundary Conditions

- Fuel gases (including moisture) are at 573 K[8], with the flux determined from the peak pyrolysis system weight loss and modeled as a volumetric source
- With the calculated φ, the mass flux of air is determined and enters at 300 K and atmospheric pressure
- Internal temperatures of the firebox brick, insulation, heat extraction tubes, and steel walls are based upon observations and simplified convective heat transfer calculations

Benchmark Results

Figure 3: Internal Temperatures of Test Data vs. Simulations

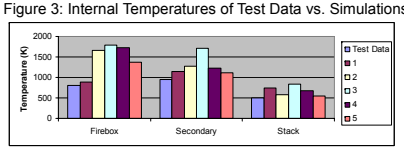

Figure 4: Stack Species Concentrations of Test Data vs. Simulations*

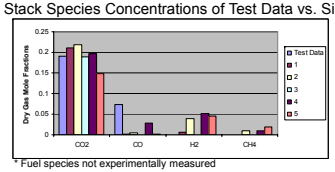

* Fuel species not experimentally measured

Benchmark Results - continued

Table 2: Comparative Summary of Benchmark Modeling Results

Run	Pros	Cons
1	• Quick convergence yields reasonable agreement with data	• Loss of in-plane gradients • Overestimation of k and ε in 2D • Difficulty in modeling tube bank
2	• Simplicity of single-species fuel yields stable solutions in less time than other 3D runs	• Equilibrium chemistry approach overestimates internal temperatures and CO oxidation • Captures flame quenching only through use of arbitrary Rich-Flammability Limit
3	• Pyrolysis mechanism models influence of wood surface radiation over fuel emission rate providing a more realistic distribution of volatilization	• Arbitrary ceiling needed to prevent runaway pyrolysis • Requires reduced enthalpy under-relaxation factor slowing solution greatly • Does not allow for direct matching of observed to simulated mass burn rate
4	• Mixture based fuel yields better agreeing exhaust CO concentrations	• Has drawbacks of run 2 with less experimentally accepted fuel composition and is less stable
5	• Finite-rate chemistry better captures the turbulent mixing-limited reaction physics and internal temperatures compared to run 4	• Unsteady solution requires a much longer simulation (+5,000 iterations)

Operational Modifications

Initial test data and analysis suggest that **the furnace is oxygen starved the first hour of the burn**. The simulation method of Run 1 is used to determine the effect of increased firebox air at peak pyrolysis for a cordwood burn, where cordwood is an unsplit log segment used in typical operation.

Figure 5: Internal Temperatures of Test Data and Simulations vs. Mass Air-to-Fuel Ratio

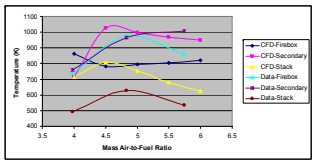

Figure 6: Mixture Fraction Variance Along Entrance to Tube Bank

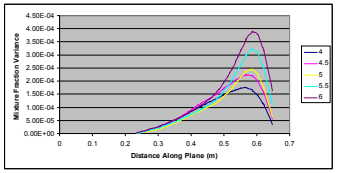

Figure 5 shows peak pyrolysis internal temperatures of simulations and test data, using a variable speed draft induction fan, versus the system mass air-to-fuel ratio, assuming the Douglas Fir is chemically approximated as $C_{4.36}H_{6.30}N_{0.01}O_{2.53}$[5]. Firebox temperatures spike in the vicinity of stoichiometric ratio of 4.78, but secondary temperatures rise beyond this point. With the increasing mixture fraction variance along the plane prior to the tube bank in Figure 6, **these indicate mixing-limited post-combustion**. However, **Test Method 28 PM emissions were reduced by 29%.**

Physical Modifications

Addressing oxygen starvation reduced thermal efficiency, as evident by increased stack temperatures and reduced heat output. It also highlighted mixing problems in the firebox and post-combustion zone, which the latter is extended by virtue of a tube bank redesign from parallel-flow to cross-flow, as seen in Figure 7. This allows for implementation of flow obstructions, i.e. baffles, and overfire secondary air injection from a hollow shelf, or 'airbox'.

Figure 7: Physically Modified Furnace

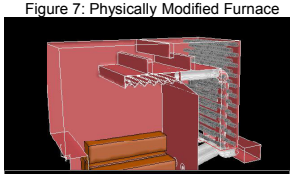

Flow visualization with inert particles is used to evaluate differing baffle configurations. Figure 8 illustrates the comparison between flush and non-flush baffles (with respect to the vertical midpoint) for pathlines and particles, colored by velocity magnitude (lower scale) and x-velocity (upper scale) respectively.

Figure 8: Pathlines and Particle Locations for Baffle Configurations

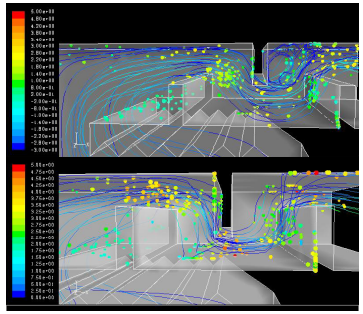

A full reacting simulation is performed, using the method of Run 5, on the modified furnace of Figure 7. Flush baffles were used, as particle residence times and circulation were greater and the pressure drop was 0.096" WC less. Due to the secondary air injection, a 120 cfm blower is used. The solution showed trace concentrations of fuel species as compared to Figure 4, and an order of magnitude improvement of the turbulent eddy mixing time scale shown in Figure 9. **Experimental tests (crib) verify the predicted improvement in combustion efficiency**, including a reduction of stack temperature to 365 K, test duration up to 295 minutes, and a thermal efficiency of 46.8%. **PM sampling has not been performed, but is reductions are expected.**

Figure 9: Turbulent Mixing Along Entrance to the Tube Bank

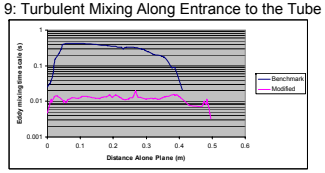

References: (1) Kronenburg, A.; Bilger, R.W.; Kent, J.H.; *Combustion and Flame*, **2000**, *121*, 24-40. (2) Tillman, D.A.; Rossi, A.J., Kitto, W.D.; *Wood Combustion: Principles, Processes, and Economics*; Academic Press: New York, NY, 1981. (3) Fine, P.M.; Cass, G.R., Simoneit, B.R.T.; *Environmental Science Technology*, **2001**, *35*, 2665-2675. (4) Fitzpatrick, E.M.; Ross, A.B., Bates, J.; Andrews, G.; Jones, J.M.; Phylaktou, H.; Pourkashanian, M.; Williams, A.; *Process Safety and Environmental Protection, Institution of Chemical Engineers*, **2007**, *85 (B5)*, 430-440. (5) Bain, R.L.; Amos, W.A.; Downing, M.; Perlack, R.L.; U.S. Department of Energy, National Renewable Energy Laboratory, *Biopower Technical Assessment: State of the Industry and Technology*, 2003. (6) *FLUENT 6.3 User's Guide*, 2006. (7) Shaskar Dixit, C.S.; Paul, P.J.; Mukunda, H.S.; *Biomass and Bioenergy*, **2006**, *30*, 684-691. (8) Huttenen, M.; Saastamoinen, J.; Kilpinen, P.; Kjällstrand, L.; Oravainen, H.; Boström, S.; *Progress in Computation Fluid Dynamics*, **2006**, *6*, Nos. 4/5, 200-208. (9) Galgano, A; Di Blasi, C.; *Progress in Computation Fluid Dynamics*, **2006**, *6*, Nos. 4/5, 287-302. (10) Bilger, R.W.; *Combustion Science and Technology*, **1976**, *13*, 155-170. (11) Magnussen, B.F.; Hjertager, B.H.; *16th International Symposium on Combustion, The Combustion Institute*, **1976**.